IEEE Open Journal of
Vehicular Technology

Received 26 March 2021; accepted 8 September 2021. Date of publication 16 September 2021;
date of current version 18 October 2021. The review of this article was coordinated by Editor Alvin Chin.

Digital Object Identifier 10.1109/OJVT.2021.3112687

An Efficient PCB Based Magnetic Coupler Design for Electric Vehicle Wireless Charging

ALI RAMEZANI (Student Member, IEEE), AND MEHDI NARIMANI (Senior Member, IEEE)

Electrical and Computer Engineering, McMaster University, Hamilton, ON L8S 4L8, Canada

CORRESPONDING AUTHOR: Ali Ramezani (e-mail: ramezana@mcmaster.ca).

This work was supported in part by the Natural Sciences and Engineering Research Council of Canada (NSERC), Discovery Grant.

ABSTRACT This paper proposes an efficient Printed Circuit Board (PCB) design of magnetic couplers for electric vehicle (EV) wireless power transfer (WPT) system. Since a WPT system operates at high frequency, Litz wire typically is used that can overcome high AC resistance, and improve overall efficiency. In EV wireless charging applications, the power level of the system is high, and therefore the magnetic pad size and copper cross-section of the Litz wire used in the magnetic couplers are large which increases the cost and weight. Besides, building the magnetic couplers using Litz wire requires excessive labor work, which causes fabrication errors. Replacing the Litz wire with PCB-based coils raises design and efficiency challenges. A new approach for designing the PCB-based magnetic couplers for high-power EV wireless charging applications is proposed to address the challenges associated with the PCB designs. In the proposed design, the efficiency of the PCB-based design is close to the Litz wire-based design. Moreover, machine assembly replaces the labor work and the magnetic coupler can be implemented with lower fabrication error, weight, and manufacturing cost. In this paper, a 3.3 kW PCB-based WPT system is designed, compared experimentally with the Litz wire setup which achieved a competitive efficiency profile.

INDEX TERMS EV wireless charging, PCB-based magnetic couplers, wireless power transfer.

I. INTRODUCTION

Wireless Power Transfer (WPT) based on inductive coupling is a suitable alternative for the conventional conduction Electric Vehicle (EV) chargers. A typical EV wireless charging system is shown in Fig. 1. As can be seen from Fig. 1, the transmitter (primary) side coil generates an alternating magnetic field coupled with the receiver (secondary) side coil. Since a wireless EV charging system operates at high frequency (i.e., 85 kHz), the magnetic couplers are typically designed based on the Litz wire [1]–[3] to reduce AC resistance, improve quality factor, and thus improve the overall efficiency of the EV charging system.

In recent years, planar magnetics attract a lot of attention due to increase power density in power converters. Planar magnetics typically have a higher surface-to-volume ratio compared to conventional magnetics. Planar magnetics use a Printed Circuit Board (PCB) instead of wire-wound coils. For example, in a PCB-based transformer, the repeatability of the design is increased, and manufacturing errors are eliminated [4]. Additionally, the parasitic elements are controllable, predictable, and consistent [5]. Similar to the transformers, the magnetic couplers (loosely transformer) of the WPT system can be replaced by a PCB layer. The idea of using PCBs for building wireless charging pads is studied for low power applications in [6]–[9]. For instance, in [10], a single-layer board is used to build spiral magnetic couplers for cell-phone battery charging applications. The maximum efficiency of the system is reported 57% due to high-frequency operation and high coil resistance. In another example [11], a double-layer spiral PCB coil is designed. The effect of the track width, copper thickness, and other board parameters on the coil resistance and its resonance frequency are studied; where the objective is to reduce the power loss for a low-power WPT system operating at 4 MHz. However, due to the high-frequency operation, the power level is limited to low power applications.

Although the PCB magnetic coupler can improve the power density, simplify production, and reduce the labor work, its application is limited to low-power WPT systems. The main challenges and limiting factors for moving toward the high-power applications are coil AC resistance due to

FIGURE 1. A typical EV wireless charging system based on inductive coupling.

high-frequency operation, thermal management due to conduction loss, and the large size of the coil. To the best of the author's knowledge, these challenges have not been studied before for using a PCB layer for high-power EV wireless charging applications. Moreover, the PCB coil design parameters have not been studied well in the aforementioned publications.

In this paper, the conventional Litz wire magnetic coupler is replaced by a PCB layer for EV wireless charging applications. This paper focuses on high power EV wireless charging application operating at 85 kHz. The effect of the ferrite material in the structure of the proposed PCB-based magnetic coupler is studied in detail. The PCB layer is analyzed using Finite Element Analysis (FEA) software to calculate the AC resistance at the operating frequency. The 2-Dimensional (2D) FEA studies are presented to provide a guideline for designing the PCB-based magnetic couplers. In this study, different factors such as the effects of the copper thickness and track width, the number of the parallel branches per turn, board layer thickness, and dimensions of the ferrite core on the AC resistance are analyzed in depth. The 3-Dimensional (3D) FEA studies are also presented to validate the 2D analysis and find a PCB layout with low conduction loss.

The magnetic couplers are designed for a 3.3 kW wireless EV charging application. The efficiency of the conventional and proposed PCB-based wireless charging systems are compared through simulation and experiments. The proposed PCB-based magnetic coupler design showed a low AC resistance and competitive efficiency compared to the Litz wire based magnetic coupler design.

II. MOVING TOWARD THE PCB MAGNETIC COUPLER FOR EV WIRELESS CHARGING AND DESIGN CHALLENGES

The efficiency and maximum transferable power of a typical induction power transfer (IPT) system are dependent on the quality factor (Q) of the magnetic couplers and the coupling factor (k) between the primary and secondary side coils. The quality factor of the primary (transmitter) and secondary (receiver) side coils of the Loosely Coupler Transformer (LCT) defined by $Q_p = \omega L_p/r_p$ and $Q_s = \omega L_s/r_s$, respectively. In this equation, ω is the angular switching frequency of the inverter in the transmitter side and r_p and r_s are the primary and secondary side coil AC resistances at the frequency of ω. Typically, as the value of $k \times Q$ increases, the system efficiency will increase [3].

A. CONVENTIONAL MAGNETIC COUPLER DESIGN FOR EV APPLICATIONS

The switching frequency for a light-duty EV wireless charger is set to 85 kHz according to the SAE standard [12]. At this frequency, due to the skin effect, the AC resistance of the single strand wire will be increased significantly compared to its DC resistance. To overcome this issue, multiple insulated strands of copper (Litz wire) are typically employed [1]. The diameter of each strand of the Litz wire is selected according to the skin depth (δ) at the operating frequency (f) and the total number of the strands (n_s) will be selected according to the total current of the wire and the desired current density (J_w). In this way, the skin effect could be mitigated and the AC resistance of the wire will be close to its DC resistance. However, due to the proximity effect, the AC conduction losses cannot be eliminated.

Fig. 2 shows the layout of a conventional rectangular magnetic pad made by Litz wire. In this structure, the total diameter of the wire D_w consists of multiple insulated copper strands with a diameter of D_s. The value of skin depth (δ) of the copper in the operating frequency determines the maximum strand diameter of each strand of the wire as follows [13]:

$$\delta = \sqrt{\frac{2\rho}{\omega\mu}} \tag{1}$$

$$D_s \leq 2\delta \tag{2}$$

where ρ is the conductor resistivity, μ is the permeability, and ω is the angular frequency. The effective cross-section area of each strand is given by:

$$S_{eff} = D_s^2 \pi / 4 \tag{3}$$

where D_s is the diameter of each strand in the Litz wire. The required cross-section area of copper based on the branch current and maximum allowable current density can be calculated as follows:

$$S_{req} = \frac{I}{J_w} \tag{4}$$

where I is the branch current and J_w is the desired current density. The current density is restricted to the maximum allowable temperature rise of the wire. The total number of strands can be selected according to the required cross-section as follows:

$$n_s = S_{req} / S_{eff} \tag{5}$$

The copper filling factor of the Litz wire, k_f, is defined by the ratio of the occupied space to the copper in the cross-section area [14]. Ideally, k_f should be one but due to the shape of the strands, strand insulation, and manufacturing process, some space of the wire will not cover by copper which results

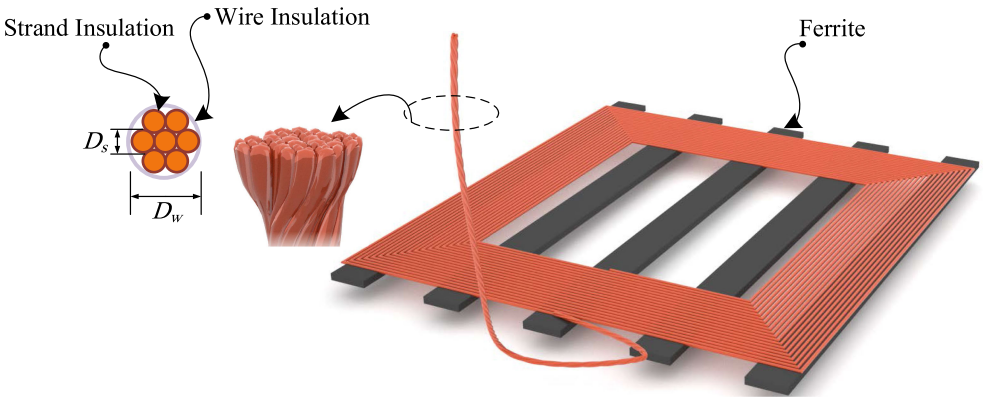

FIGURE 2. Rectangular magnetic pad made by Litz wire.

in higher k_f values. According to (1), the selected strand size should be smaller than twice the skin depth to reduce the skin effect. However, having very thin strands results in a higher value of k_f [15] that results in larger diameter wires compared to single strand wire with equivalent copper cross-section area.

It should be noted that the high value of k_f results in lower copper in a specific area which leads to a low power density design. Additionally, the availability of the Litz wires with a high number of strands and low strand diameter is another limiting factor [15]. Although the Litz wire can mitigate the skin effect and reduce the AC resistance, the cost of the Litz wire increases significantly as the number of strands increases.

Besides the significant increase in the cost of the Litz wire for high power applications, the manufacturing errors should be considered. These errors could be related to building the coil or elements of the magnetic coupler including Litz wire. In the case of using a high gauge wire for the strands (tiny strands), it is possible to have more broken strands due to their fragility [15]. Therefore, the effective number of strands will be reduced and thus increasing the conduction loss. The insulation layer of the Litz wire has some manufacturing tolerance that affects the spacing between the turns. Moreover, space between the wire and ferrite core can have some errors during manufacturing. The aforementioned problems lead us to design PCB based magnetic coupler, which will be explained in the following section.

B. THE PROPOSED PCB BASED MAGNETIC COUPLER DESIGN

1) LAYOUT

A PCB-based magnetic structure offers a higher power density and a simple manufacturing process compared to a conventional Litz wire based structures [16], [17]. The design tolerance will be limited to PCB production error which is significantly lower compared to manufacturing conventional wire-wound coils [17]. Additionally, the parasitic elements of the circuit are predictable and thus can be considered and mitigated in the analysis [5]. Moreover, the manufacturing costs will be reduced due to simplicity and machine assembly instead of labor work. Considering the advantages of the PCB-based magnetic structure over conventional wire-wound coils, a planner magnetic structure based on the PCB can be used for EV wireless charging applications.

The proposed magnetic coupler is utilizing a multi-layer PCB as shown in Fig. 3. In this structure, the wireless charging coils are printed on the board material. It is possible to have multiple layers to increase the current capability and reduce conduction loss. The layers of the structure can be connected in parallel to reduce the AC resistance. Similarly, by increasing the trace width and copper weight (copper thickness), the coil resistance can be reduced. It should be noted that different layers are insulated from each other by a dielectric material.

2) DESIGN CHALLENGES

As discussed, the quality factor of the coils should be high to ensure a high-efficiency profile for the wireless power transmission system. Since the operating frequency for EV application is restricted to 85 kHz, the self-inductance of the coil and its AC resistance are the remaining design parameters to achieve high-quality factor magnetic couplers. The self-inductance is dependent on the number of turns, the dimension of the coil, and the magnetic core material. The coil AC resistance is dependent on the copper cross-section, the spacing between the turns (proximity effect), and its length.

The size of the magnetic couplers should be optimally selected to avoid large structures. Especially for EV applications, the vehicle-side coil size is limited to the available space underneath the vehicle. Moreover, the vehicle side magnetic structure and pickup converter should be light-weight. Therefore, the core material should be optimally selected.

In a PCB-based magnetic structure, each turn can be made by a limited number of strands compared to the Litz wire based structure. Therefore, Finite Element Analysis (FEA) is required to optimally design the PCB-based structure and select the track width (T_w) and the number of parallel branches (N_{br}). Moreover, the current capability of the PCB tracks is limited due to the coil conduction loss. Having high conduction loss on the coils reduces the efficiency of the system and

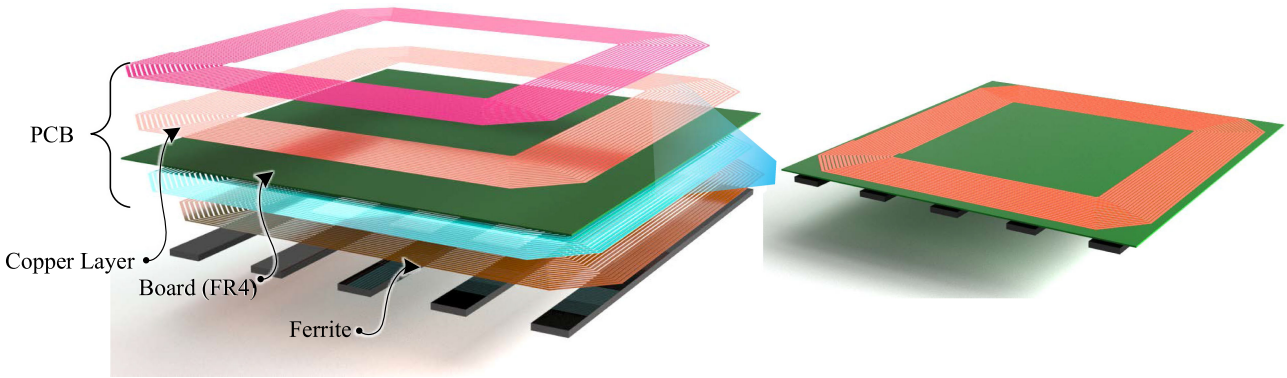

FIGURE 3. The proposed magnetic pad made by multi-layer PCB.

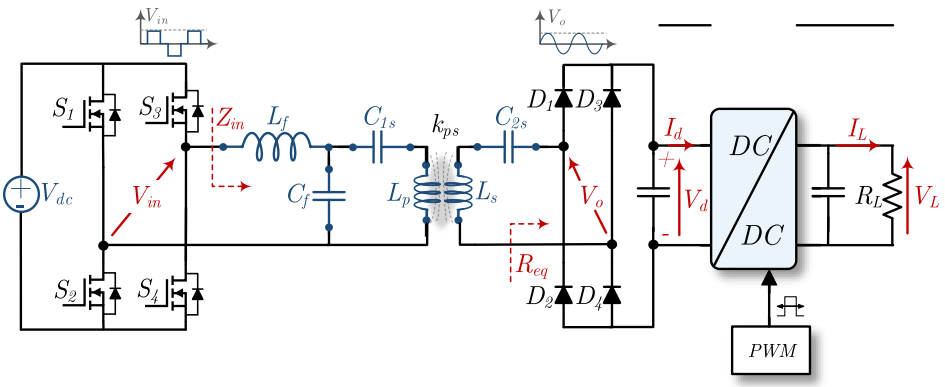

FIGURE 4. Circuit diagram of the LCC-S compensated WPT system and battery control scheme.

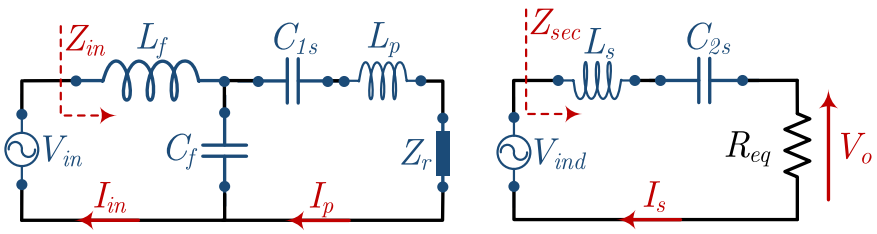

FIGURE 5. Equivalent circuit of LCC-S topology according to fundamental harmonic approximation.

may violate the allowable temperature of the board material. These design challenges are addressed in Section III.

3) CIRCUIT MODELING

In this paper, an LCC-S topology is selected for the compensation network of the IPT system according to [18], [19]. The simplified circuit schematic is shown in Fig. 4. In this system, S_1-S_4 are power switching semiconductor devices of the full-bridge inverter that are controlled by phase-shifted modulation. In this circuit, k_{ps} is the mutual inductance of the main magnetic couplers. On the vehicle side, the output of the diode bridge can be connected to a buck or boost type DC-DC converter to charge the battery in both Constant Current (CC) and Constant Voltage (CV) modes. By using the Fundamental Harmonic Analysis (FHA), the circuit schematic could be further simplified as shown in Fig. 5 where p refers to the main primary coil (L_p), s refers to the main secondary coil (L_s).

When the circuit is excited with the resonant frequency, the secondary side circuit impedance will be eliminated ($L_sC_{2s}\omega^2 = 1$) and the output voltage will be equal to the induced voltage. In this condition, the output voltage is independent of the load variation and the voltage source feature of the LCC-S network is achieved. Having an LCC compensation on the primary side generates a constant current in the primary coil. Therefore, the total conduction loss of the primary side will remain constant in the charging process. In this case, a slight change of the r_p results in a high variation of efficiency which is leading to higher sensitivity at light load conditions.

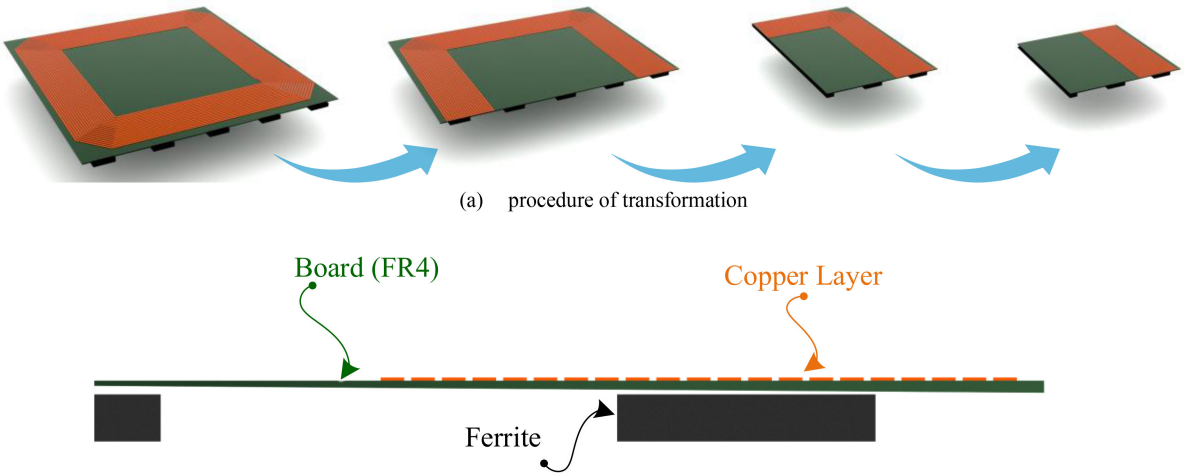

FIGURE 6. Simplification of the 3D model to a 2D model.

However, by designing the circuit to achieve a low current and high voltage on the secondary side, the conduction losses will be reduced, and coil resistance (r_s) has a negligible effect on system efficiency. Therefore, instead of the high-cost Litz wire based magnetic coupler, other alternatives such as the proposed PCB-based magnetic structure could be used for the secondary side coil.

III. PCB BASED MAGNETIC COUPLER DESIGN

In this paper, a rectangular Litz wire based magnetic structure is considered. The conventional magnetic structure, as studied in [20], is used as a benchmark to evaluate the proposed PCB-based magnetic structure. The power rating, input, and output voltage, and misalignment range are considered to be the same for both systems. The coil AC resistance and self-inductance are considered as a figure of merit in this section.

To design the PCB-based structure, 3D-FEA studies are required. However, due to the computationally intensity and complexity of the modeling, 2D-FEA studies are employed first. The 2D-FEA study illustrates the effectiveness of each design parameter that leads to minimum coil resistance. The result of the 2D analysis will be used to design the 3D model for further evaluation. Accordingly, the optimal design is selected and misalignment analysis is performed. Finally, the PCB design is compared with the reference design built by Litz wire.

A. TWO-DIMENSIONAL STUDIES

In order to have a fair comparison, the range of the design variables of the PCB structure is selected to be in the range of the reference design which is a coil made by Litz wire. Therefore, the total coil width is 80 mm, and the PCB coil has 20 turns on each layer. Fig. 6 illustrates the procedure of generating the equivalent model of the 3D structure for 2D studies. In this study, the frequency is swept from 10 Hz to 200 kHz to study the skin effect on the coil resistance. This procedure is repeated for boards with 1 to 4 layers.

In this section, different magnetic coupler design parameters that affect the coil AC resistance are studied. The objective of this analysis is to find the best magnetic coupler design with minimum AC resistance. These parameters are listed as follows:

1) Copper cross-section
2) Number of parallel branches
3) Dielectric layer thickness
4) Magnetic core material

1) COPPER CROSS SECTION

In a solid conductor, as the cross-section area increases, the DC resistance decreases. However, due to the skin effect, the AC resistance of the wire will not decrease as the cross-section increases. To evaluate the effect of the track cross-section on the coil resistance, the copper track width (T_w) and copper weight (T_{cu}) is changed in the range of 0.5-3.5 mm and 1-6 oz, respectively. In this part, the ferrite core is not considered to only the effect of the copper cross-section on the AC resistance is studied. The effect of the ferrite material is studied in the next part. Fig. 7 shows the FEA results of the coil resistance per meter (Ω/m) versus the copper cross-section for one, two, and four-layer boards. It can be seen that generally the coil resistance will be reduced as the copper thickness increases. However, the effect of copper thickness will be negligible as the track width is high enough. Moreover, as the number of layers increases, the AC resistance of the coil decreases. However, the designs with a track width of larger than 1.5 mm showed negligible changes to the number of layers and copper weight increase. Therefore, the coil quality factor will not benefit from having an excessive number of layers. Additionally, the lower number of layers is preferable

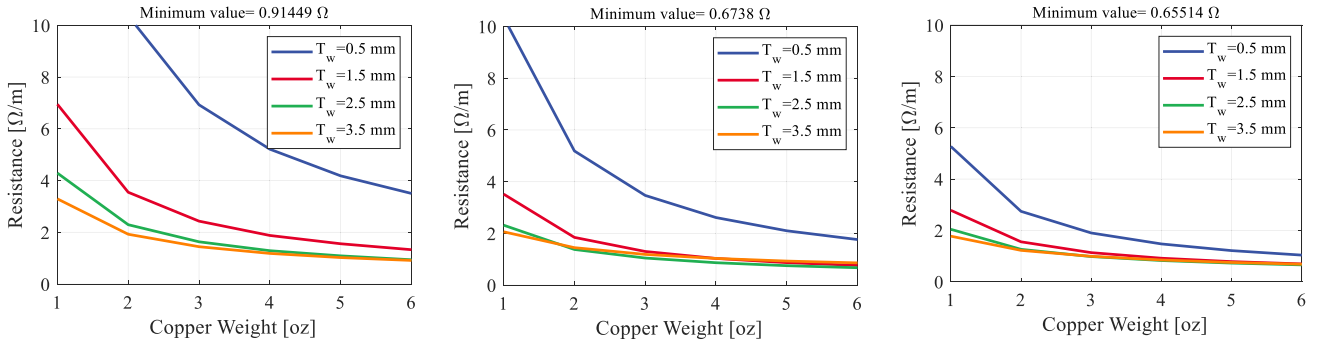

(a) 1-Layer board (b) 2-Layer board (c) 4-Layer board

FIGURE 7. Track AC resistance per meter versus copper thickness at different track width: (a) 1-Layer board (b) 2-Layer board (c) 4-Layer board.

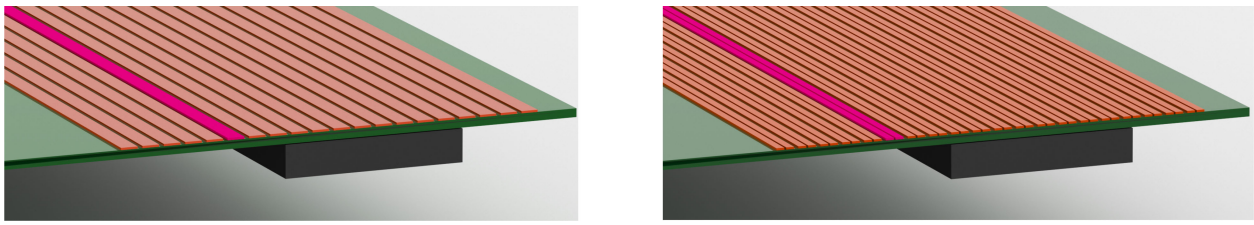

(a) single branch for each turn (b) two parallel branches for each turn

FIGURE 8. Coil turns layout with parallel branches.

due to the high cost of multi-layer PCB designs. This could be achieved by the optimal design of the copper layer.

2) PARALLEL BRANCHES

Similar to the Litz wire design, the PCB tracks could be designed. In this way, each turn of the coil is divided into multiple parallel branches (N_{br}) as shown in Fig. 8. In this part, designs with a different number of parallel branches are considered to study their effect on the coil AC resistance. Since the skin depth at 100 kHz is around 0.2 mm, the width of parallel branches should be selected close to 0.4 mm according to (2). Similar to the previous part, single-layer, two-layer, and four-layer board layouts are considered and the FEA results are shown in Fig. 9.

By comparing the FEA results between the cases with two and three branches, it can be seen that the changes in the minimum achievable value are negligible. It should be noted that the designs with track width smaller than twice the size of the skin depth are showing the highest resistance even at high copper weights (copper thickness). It can be seen that as the branch width is larger than 0.4 mm, the resistance of the coil is reduced significantly. However, beyond the 0.4 mm track width, the changes are negligible and the reduction rate of the resistance versus copper weight and track width is saturated. Furthermore, the designs with a 0.2 mm track width showed higher changes when the number of parallel branches is increased.

Comparing the presented results in Fig. 9 to the single branch layout (Fig. 7), it can be seen that when the copper cross-section is lower than twice the skin depth in each direction, having a higher number of parallel branches (N_{br}) is beneficial. A design with a low copper cross-section can be selected in two scenarios: cost limitation, and space limitation. In any of these cases, the presented results could be helpful for the designer to appropriately select the optimal sizes for the copper layer of the coils. As the copper cross-section or number of layers increases, the parallel branches' effect on the coil resistance is reduced.

Moreover, it can be seen that the minimum achievable resistance for a single branch per turn is lower than multiple parallel branches. This pattern can be seen in all the number of layers. Because of the restriction of the coil total width to 80 mm (to match the reference Litz wire design), as the number of branches increases, the clearance between the branches and different turns will be reduced. It should be noted that in the high-power application, the clearance between the turns is essential to avoid insulation issues. Therefore, the proximity effect will be increased, and the coil AC resistance per meter will be increased compared to the single branch case presented in Fig. 7. Depending on the requirements of each application, the designer can select the optimal value of the coil width to minimize the coil AC resistance. In this paper, a comparable equivalent for the reference Litz wire based magnetic coupler is considered as a baseline.

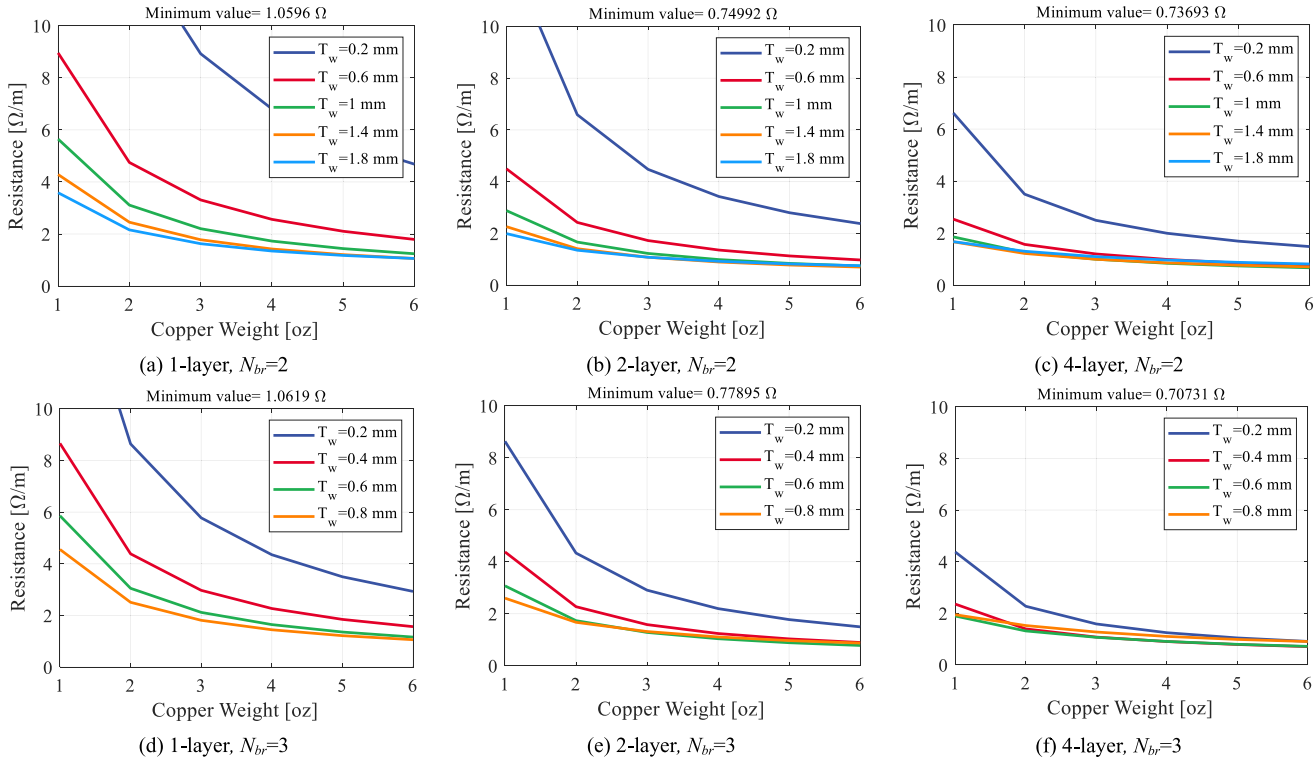

FIGURE 9. Track AC resistance per meter versus copper weight at different branch width: (a) 1-Layer board with 2 parallel branches (b) 2-Layer board with 2 parallel branches (c) 4-Layer board with 2 parallel branches (d) 1-Layer board with 3 parallel branches (e) 2-Layer board with 3 parallel branches (f) 4-Layer board with 3 parallel branches.

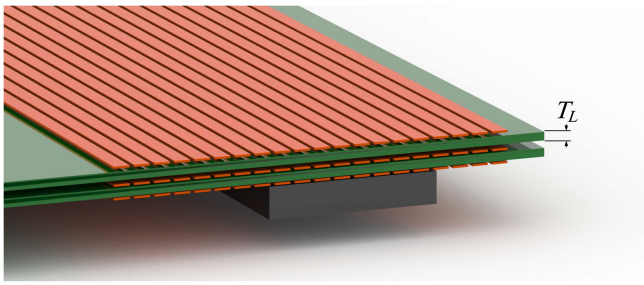

FIGURE 10. Layer thickness in a multi-layer board.

3) LAYER THICKNESS

Due to the proximity effect at high-frequency operation, the AC resistance of the coils could be affected by nearby turns and layers. The layer insulation thickness (T_L) is considered as another design variable in this part as shown in Fig. 10. In this study, the dielectric thickness is varied from 0.2 mm to 1.8 mm, and copper thickness (T_{cu}) is changed between 3–6 oz. The branch width is changed between 1.5–3.5 mm, 0.6–1.8 mm, and 0.4–0.8 mm for the single branch, two branches, and three branches designs, respectively. The FEA results of this study for two branches are presented in Fig. 11 with the same color maps as Fig. 7.

In Fig. 11, the results for 0.5 mm and 0.2 mm are not presented due to high coil resistance per meter (dark blue curves). According to Fig. 11, it can be seen that in all types of designs with different copper weights (T_{cu}), the coil resistance is reduced as the spacing between the layers (T_L) reduces. However, as the branch width (T_w) is increased, the variation of the AC resistance versus the layer thickness is increased. However, the changes in the 6 oz designs are close to the 3 oz designs. In another word, the coil resistance is more sensitive to the board layer thickness when wider tracks are used. According to Fig. 11, having wider branches does not necessarily result in lower resistance. It can be seen that the resistance of the designs with $T_w = 1.8$ mm is higher than the designs with $T_w = 1.4$ mm due to the proximity effect as discussed in part 2.

Another important point that can be seen is that by changing the copper thickness from 3 oz to 6 oz the resistance of the design with 3.5 mm is increased beyond the resistance of the 1.5 mm track width design. Having higher copper thickness significantly increases the production cost; it was shown that it can be nullified if the layer thickness is not selected optimally. Moreover, changing the thickness of the board typically does not affect the production cost. Therefore, the optimal selection of the board thickness is a vital step in designing the PCB magnetic couplers. It should be noted that the effect of layer thickness is only observed on the high-frequency excitation of the coils. The coil resistance under DC or low-frequency operation remains constant versus layer thickness.

Similarly, the 4-layer PCB layout is studied and similar results are achieved. By reducing the layer thickness the coil

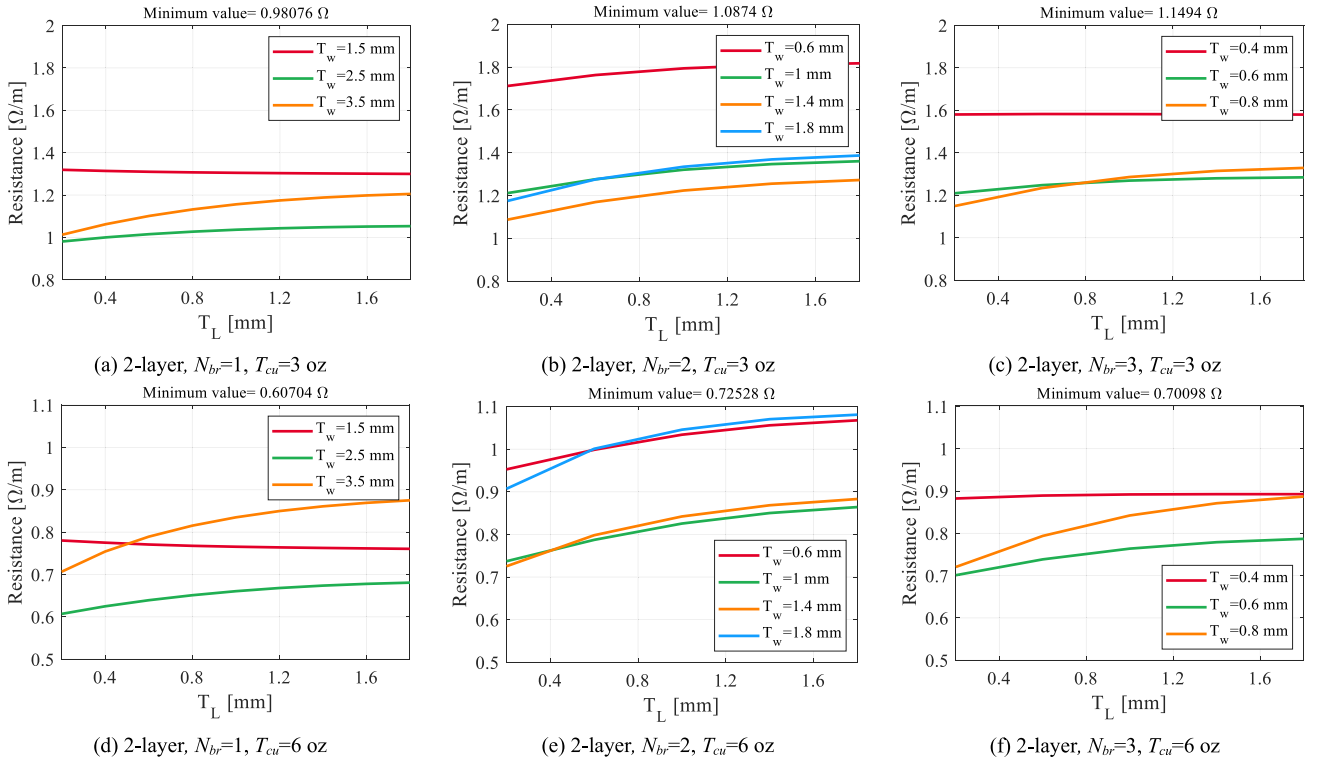

FIGURE 11. Track AC resistance per meter versus layer thickness at different branch width of a 2-layer board: (a) single branch with 3 oz copper weight (b) two branches with 3 oz copper weight (c) three branches with 3 oz copper weight (d) single branch with 6 oz copper weight (e) two branches with 6 oz copper weight (f) three branches with 6 oz copper weight.

AC resistance is reduced. Additionally, the minimum possible AC resistance is around 0.54 Ω/m corresponding to the 4-layer board with a branch width of 2.5 mm and 6 oz copper thickness. Although the 2-layer board showed a comparable low resistance at the same design point (Fig. 11(e)), other parameters such as current density and temperature rise should be considered in practice.

4) MAGNETIC CORE MATERIAL

Magnetic core material such as Ferrite can be added to the magnetic couplers to improve the coupling factor, increase the self-inductance and quality factor, and reduce the field emission in the backside of the magnetic couplers. Due to the high permeability of the ferrite, adding this to the magnetic structure can change the magnetic field distribution. Changes in the magnetic field could result in the variation of the coil resistance due to the eddy current effect. Therefore, in this part, the ferrite blocks are added to the 2D analysis to investigate their effect on the AC resistance of the coil at the operating frequency. In this study, different thickness of ferrite material (T_f) is placed underneath the board and FEA is performed on the 2D model. To save space, as an example, the FEA results for a single branch and 3 branches layouts with the board thickness of 0.2 mm and 6 oz copper thickness are presented in Fig. 12.

As can be seen, the ferrite core has a negligible effect on the coil AC resistance at this frequency. Generally, having ferrite blocks in the structure leads to slightly higher AC resistance. Although introducing the ferrite material will change the magnetic field distribution around the ferrite blocks, the changes in the coil resistance are not large. This is because of the fact that the size of the core is smaller compared to the air surrounding the magnetic couplers.

B. THREE-DIMENSIONAL STUDIES

Based on the presented 2D-FEA results, the 3D design (Fig. 3) parameters can be selected optimally. The 2D FEA results provided the guidelines to optimize the PCB layout of the magnetic couplers. For instance, the effect of the parallel branches and board dielectric thickness on the coil AC resistance is studied in the 2D modeling and the conclusions can be applied to the 3D model. In this way, the computation time and complexity are reduced.

It should be noted that these designs are restricted to the same outer and inner dimensions of the reference Litz wire structure. Therefore, a fair comparison between the two cases can be done. In this paper, several iterations are done to find one of the optimal designs which are suitable for EV charging application. To avoid paper overlength, only a few numbers of 3D iterations are presented in this part as an example.

1) COPPER CROSS-SECTION

The effect of the copper cross-section on the current density distribution (**J**) of a 10 A current excitation with the frequency

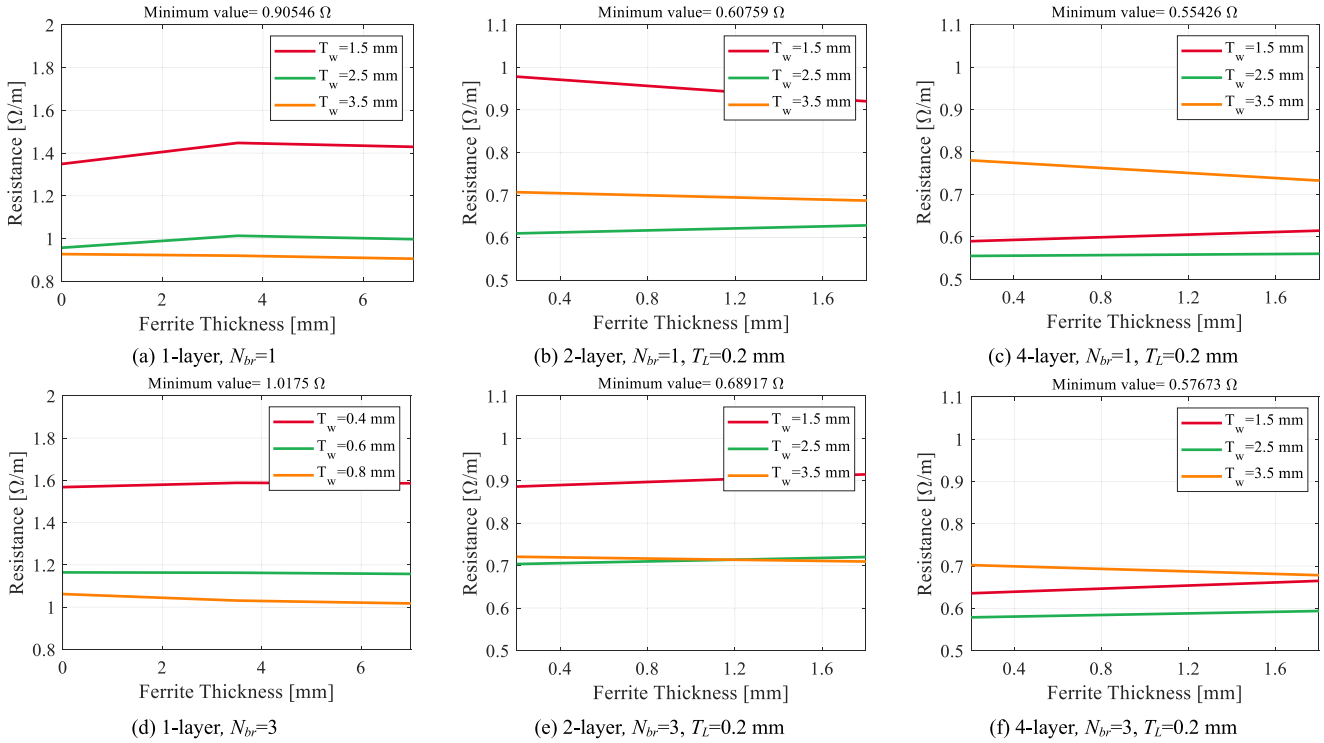

(a) 1-layer, N_{br}=1 (b) 2-layer, N_{br}=1, T_L=0.2 mm (c) 4-layer, N_{br}=1, T_L=0.2 mm

(d) 1-layer, N_{br}=3 (e) 2-layer, N_{br}=3, T_L=0.2 mm (f) 4-layer, N_{br}=3, T_L=0.2 mm

FIGURE 12. Track AC resistance per meter versus ferrite thickness at different branch width: (a) 1-Layer board with single branch (b) 2-Layer board with single branch (c) 4-Layer board with single branch (d) 1-Layer board with 3 parallel branches (e) 2-Layer board with 3 parallel branches (f) 4-Layer board with 3 parallel branches.

of 100 kHz is illustrated in Fig. 13. In this figure, only one corner of the 3D model is shown for better visibility of the results. It can be seen that as the copper thickness (T_{cu}) increased, the current density is reduced and the surface of the maximum current density is reduced. Moreover, it can be seen that as T_{cu} increased, the proximity effect is reduced. Therefore, having a higher copper weight can be beneficial to avoid hotspots in the PCB-based magnetic structure.

When the track width (T_w) and increased from 1 mm to 1.5 mm, the current density is distributed more evenly. Up to 2.5 mm track width, similar behavior is observed. However, beyond the track width of 2.5 mm, the proximity effect caused higher current density in the corners of the track as shown in Fig. 13(e) and (g), and (f) and (h). This result is similar to the presented results for a 4-layer board. The calculated AC resistance at 100 kHz of the presented designs and the minimum values for 6 oz copper thickness is shown in Fig. 14.

2) LAYER THICKNESS

In this part, the effect of the dielectric thickness (T_L) on the AC resistance of the actual 3D model is studied. Similar to the 2D studies, a reduction of the coil AC resistance versus T_L is observed. As an example, the current density of a 4-layer PCB layout with a dielectric thickness of 0.7 mm and 0.2 mm is shown in Fig. 15(a) and (b), respectively. It can be seen that there are fewer points that have a current density of 30 A/mm^2 and beyond in the layout with a 0.2 mm layer dielectric thickness. The AC resistance of the coils is also dropped from 1.78Ω to 1.105Ω when the layer thickness is reduced which is close to a 30 % reduction of the resistance similar to Fig. 11.

TABLE 1. Selected Magnetic Coupler Specifications

Parameter	Symbol	Design Value
Primary side number of turns (Litz)	N_p	20
Secondary side number of turns (PCB)	N_s	20
Copper thickness	T_{cu}	6 oz
Number of parallel branches	N_{br}	1
Track width	T_w	2.5 mm
Board dielectric thickness	T_L	0.2 mm
Ferrite Thickness	T_f	7 mm
Ferrite width	T_{fw}	35 mm

C. SELECTED DESIGN

According to the 2D analysis, 3D designs were analyzed and compared. After several iterations, an optimal design is selected and the specification is listed in Table 1. Considering the implementation cost, and 2D analysis, a four-layer PCB is selected. Based on the FEA results, one of the designs which showed the minimum AC resistance is found and selected for the magnetic structure.

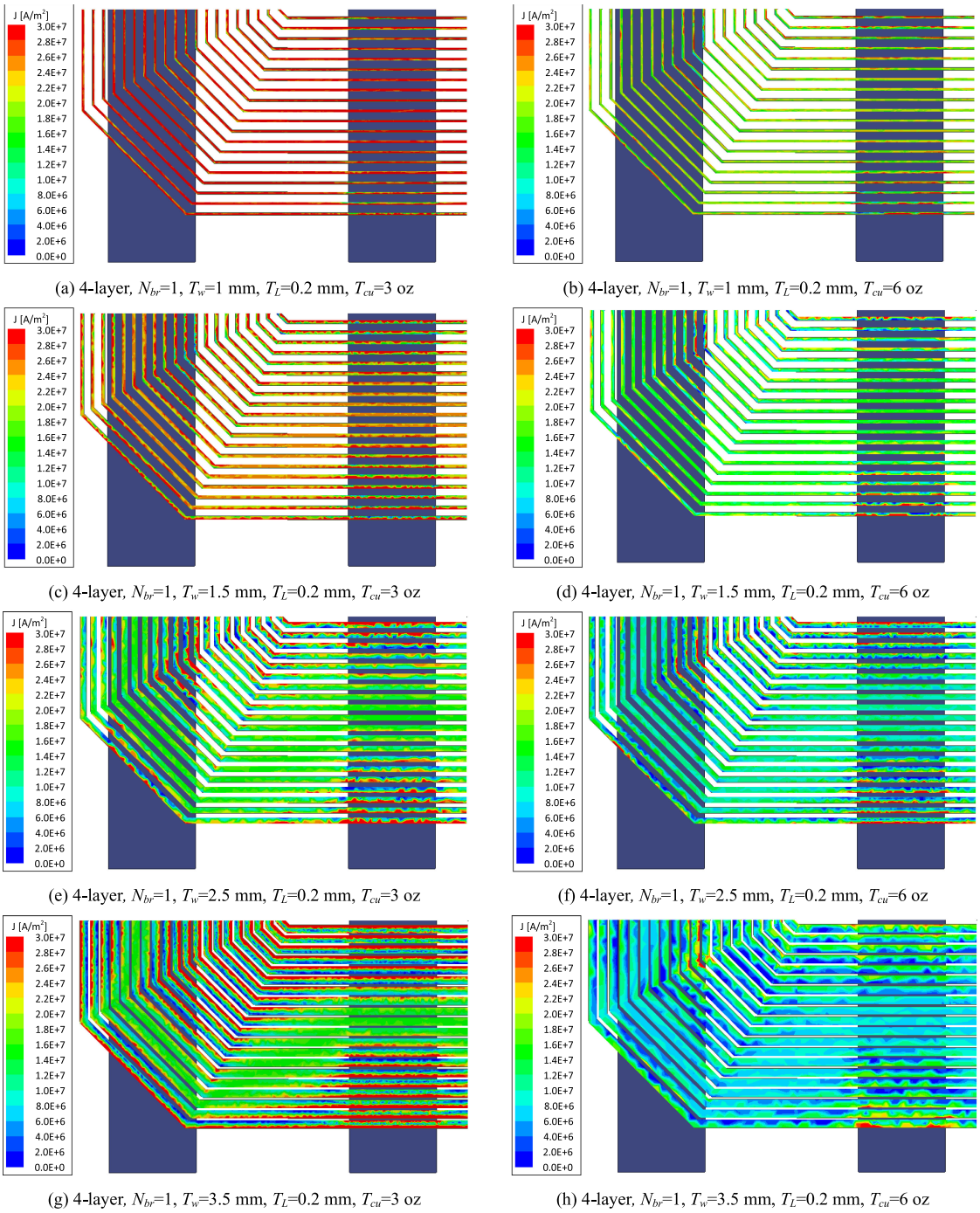

(a) 4-layer, N_{br}=1, T_w=1 mm, T_L=0.2 mm, T_{cu}=3 oz

(b) 4-layer, N_{br}=1, T_w=1 mm, T_L=0.2 mm, T_{cu}=6 oz

(c) 4-layer, N_{br}=1, T_w=1.5 mm, T_L=0.2 mm, T_{cu}=3 oz

(d) 4-layer, N_{br}=1, T_w=1.5 mm, T_L=0.2 mm, T_{cu}=6 oz

(e) 4-layer, N_{br}=1, T_w=2.5 mm, T_L=0.2 mm, T_{cu}=3 oz

(f) 4-layer, N_{br}=1, T_w=2.5 mm, T_L=0.2 mm, T_{cu}=6 oz

(g) 4-layer, N_{br}=1, T_w=3.5 mm, T_L=0.2 mm, T_{cu}=3 oz

(h) 4-layer, N_{br}=1, T_w=3.5 mm, T_L=0.2 mm, T_{cu}=6 oz

FIGURE 13. **Current density distribution in the 3D models of the 4-layer PCB.**

1) THERMAL ANALYSIS

To calculate the maximum temperature rise of the board, a steady-state 3D finite element analysis is done. Noting the symmetry of the design, a 50 mm cut of the board is considered to reduce the complexity of the simulation and required computational power. Fig. 16 shows the surface temperature of the PCB when the 10A sinusoidal current is flowing to the copper traces. In this study, the ambient temperature is assumed to be 23°C. The maximum temperature of the copper versus the RMS value of the current is calculated and the results are shown in Fig. 17. Since the board material used in this paper is T_g=180°C, the calculated values of the maximum copper temperature are in the safe operating region.

2) COMPARISON

To evaluate the proposed PCB-based magnetic coupler, the secondary side of the conventional wireless charger is replaced by the PCB, and the system efficiency is compared.

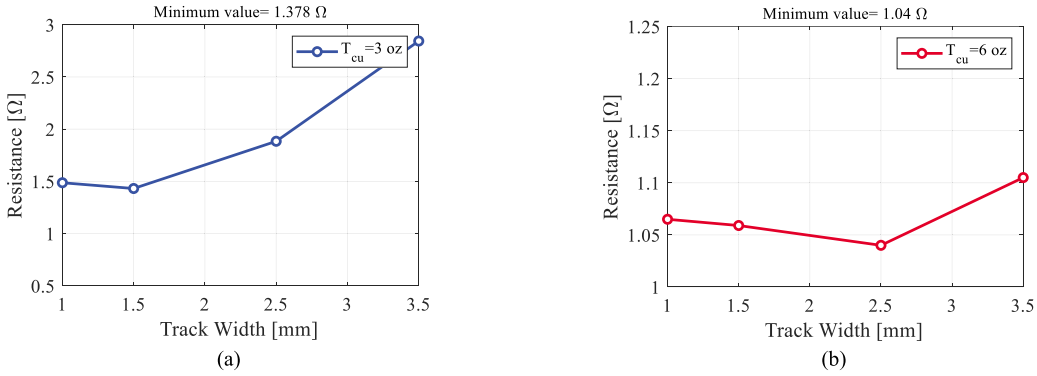

FIGURE 14. Calculated AC resistance of the single branch 4-layer PCB designs versus track width.

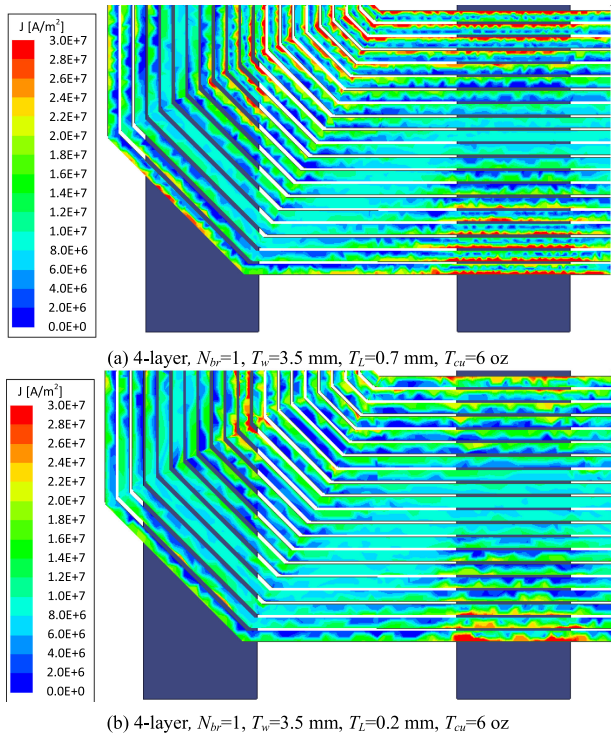

FIGURE 15. Current density in the 3D models of the 4-layer PCB.

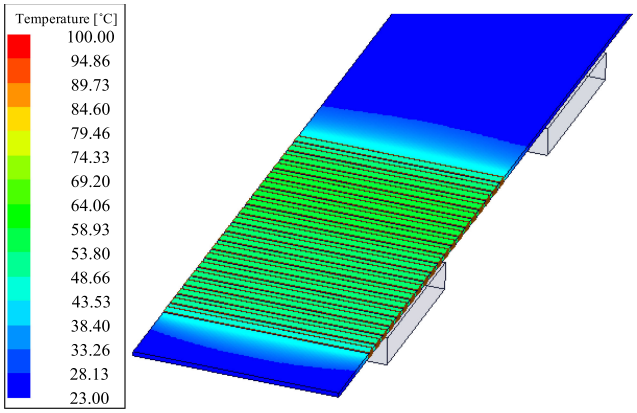

FIGURE 16. Surface temperature of the proposed magnetic coupler based on PCB flowing I_s=10 A RMS.

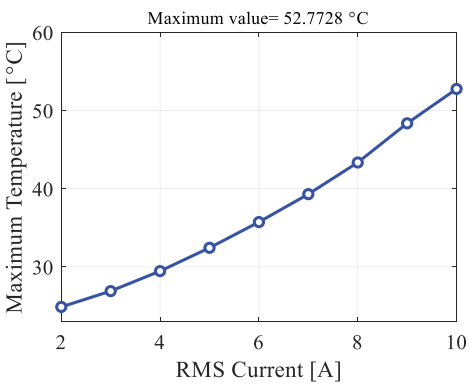

FIGURE 17. Maximum temperature of the copper versus RMS current.

The efficiency of the two systems with identical parameters except for the coil resistance versus the output power under full-aligned condition is shown in Fig. 18. It can be seen that replacing the secondary side coil with a PCB has a negligible effect on the efficiency at low power operation and at high power operation conditions, the difference is low. It is worth mentioning that the proposed PCB-based magnetic coupler can reduce the volume of the coil by 55% compared to a conventional design due to the small thickness of the coil.

IV. EXPERIMENTAL RESULTS

To evaluate the performance of the proposed magnetic coupler based on PCB, a 3.3 kW wireless power transfer system is built. The LCC-S resonant network is designed according to the optimization method presented in [19]. In this design, it is assumed that the input voltage is 200 V and the coupling factor is in the range of 0.22-0.32. The selected parameters of the LCC-S network are listed in Table 2. The efficiency and output voltage of this system will be compared in this Section.

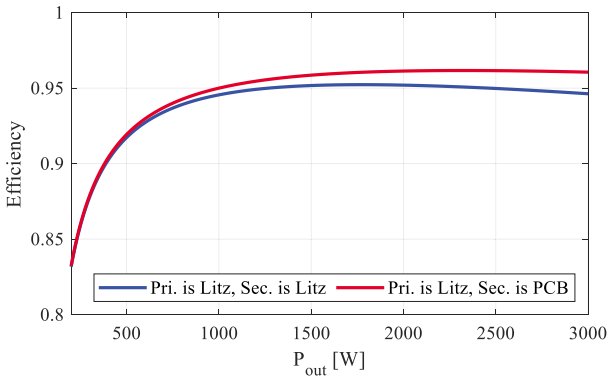

FIGURE 18. Comparison of the conventional and the proposed wireless charging systems.

TABLE 2. Resonant Network and System Specifications

Parameter	SYMBOL	Design Value
Primary side resonant inductor	L_f	49.18 μH
Primary side parallel capacitor	C_f	71.05 nF
Primary side series capacitor	C_{1s}	10.19 nF
Secondary side series capacitor	C_{2s}	9.23 nF
Maximum Power	P_{max}	3.3 kW
Nominal power range	P_n	540W~3300W
Nominal coupling factor range	K_n	0.22~0.32
Misalignment	-	±110 mm
Air gap	-	125 mm
Switching frequency	f	85 kHz
Input DC voltage	V_{dc}	200 V

In this setup, the inverter is built by IPW65R037C6 power Si MOSFET switching at 85 kHz. The diode bridge on the receiver side is built with DSEI120-06A. The output of the diode rectifier is connected to a DC-DC converter supplying the load and provide a regulated output voltage. The resonant capacitors are Metalized Film Propylene (MFP) from EPCOS with a low Equivalent Series Resistance (ESR) and high rated AC voltage withstand at 85 kHz.

The conventional Litz wire coils are built with 500 strands of AWG38 Litz wire. The four-layer PCB-based magnetic coupler is built according to the specification listed in Table 1. The magnetic couplers based on Litz wire and PCB-based magnetic coupler are shown in Fig. 19(a) and (b), respectively. The dimension of the ferrite bars is 510 mm × 38 mm × 7 mm and the material of the ferrite core is N87 from EPCOS which has core loss at the high operating frequency.

In the proposed configuration, the primary side coil is built using the Litz wire and the secondary side is built using a PCB. The measured self-inductance of the magnetic coupler made by Litz wire on the primary side, L_p, is 386.6 μH and the self-inductance of the PCB-based magnetic coupler on the secondary side, L_s, is 380.1 μH. Both the primary and secondary side pads have the same dimensions of 550 mm × 550 mm.

The output voltage of the inverter (V_{in}), inverter current (I_{in}), output DC voltage (I_d), and output DC (I_d) waveforms

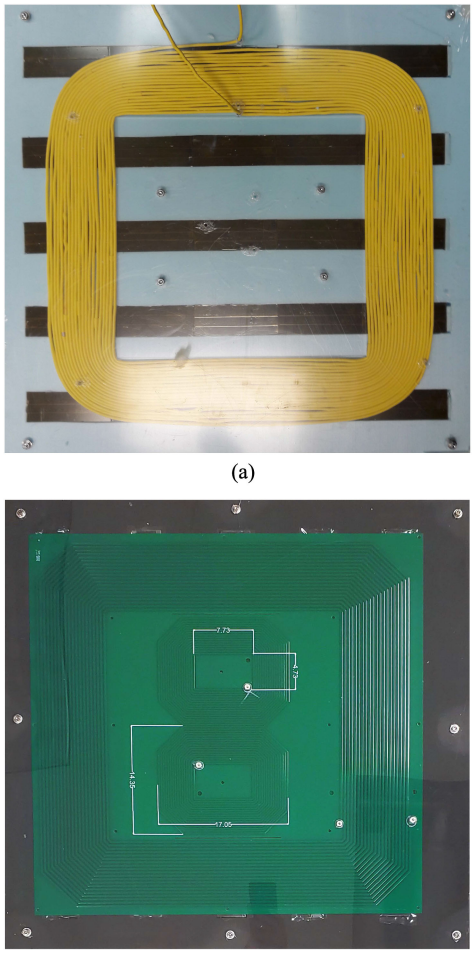

(a)

(b)

FIGURE 19. Magnetic couplers built by: (a) Litz wire (b) PCB coil.

in the aligned position under 3.3 kW and 500 W loading conditions are shown in Fig. 20. It can be seen that the Zero Voltage Switching (ZVS) is realized due to the inverter current phase lag. In another word, the current is passing through the anti-parallel diode of the MOSFET before the switching moment. Therefore, the turn-on voltage of the switch is close to zero and soft switching is realized. The efficiency of the proposed configuration is measured experimentally and compared with calculation results as shown in Fig. 21. In this figure, the measured DC to DC power efficiency is reported. It can be seen that the measured efficiency is close to the calculation results. In the next step, the proposed combination that has PCB coil on the secondary side and Litz wire on the primary side is compared with the conventional dual-side Litz wire magnetic couplers. The coil inherent quality factor comparison is presented in Fig. 22. It can be seen that the proposed PCB-based magnetic coupler, offers a competitive quality factor compared to the conventional magnetic coupler which ensures high efficiency of the proposed PCB-based magnetic coupler.

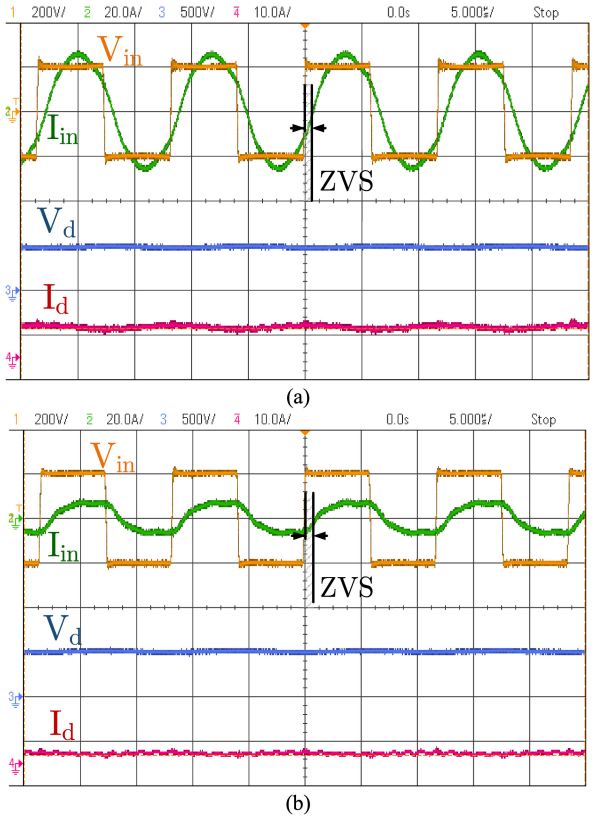

FIGURE 20. Experimental output waveforms when magnetic couplers are fully aligned: (a) 3.3 kW (b) 500 W.

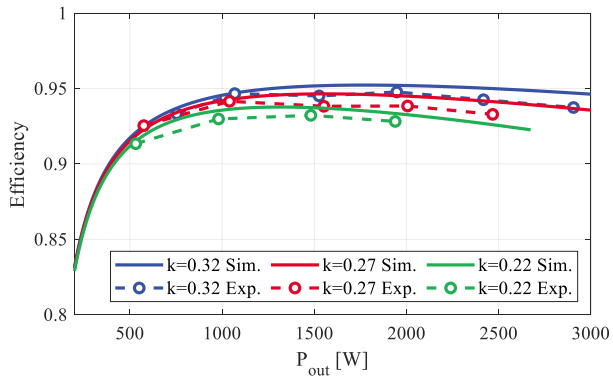

FIGURE 21. Measured experimental efficiency values versus calculation results.

In the next step, the efficiency of the proposed combination that has PCB coil on the secondary side and Litz wire on the primary side is compared with the conventional WPT system based on Litz wire on both sides. The efficiency comparison is presented in Fig. 23. It can be seen that by replacing the vehicle side Litz wire coil with the PCB-based magnetic coupler, the efficiency reduction is not considerable. Moreover, at light load conditions, the proposed PCB-based secondary coil showed a close performance to the conventional magnetic coupler based on Litz wire.

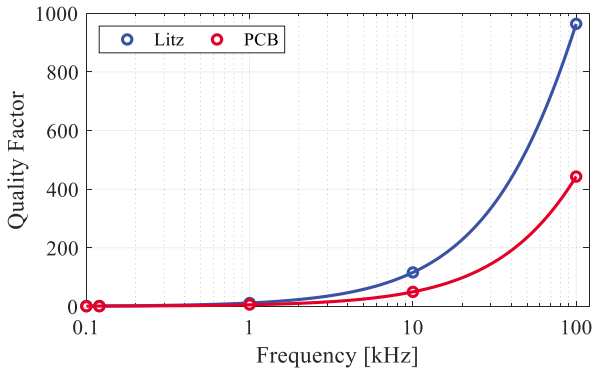

FIGURE 22. Coil quality factor comparison between the conventional magnetic coupler made by Litz wire and PCB coil on the secondary side.

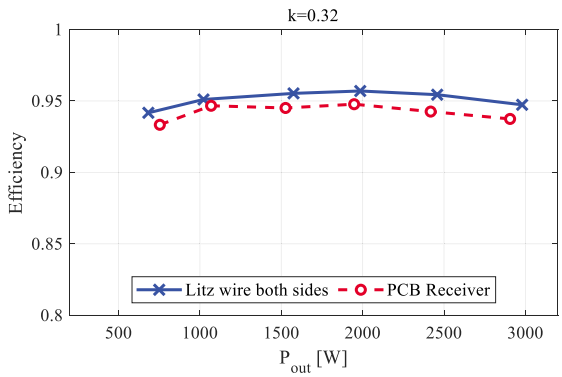

FIGURE 23. Efficiency comparison between the conventional magnetic coupler made by Litz wire and PCB coil on the secondary side.

V. CONCLUSION

In this paper, a cost-effective, simple to manufacture, and efficient magnetic coupler based on the Printed Circuit Board (PCB) is proposed. The main advantage of the proposed magnetic coupler is the reduction of weight, fabrication error, labor work, and maintaining high efficiency.

To design a competitive and efficient coil based on PCB, different design parameters are considered. In this study, copper cross-section, the number of parallel branches, dielectric layer thickness, and magnetic core effect on the AC resistance is studied. In order to evaluate the effect of each design parameter on the AC resistance of the coil, Finite Element Analysis (FEA) is presented. According to the FEA results, when the track width is smaller than twice the size of the skin depth, the design showed the highest resistance even at high copper weights. Although having multiple parallel branches resulted in lower AC resistance as the number of branches increases, the changes are not large. As the number of branches increases, the clearance between the turns will be reduced; therefore, having many parallel branches results in higher AC resistance due to the proximity effect.

The dielectric layer thickness is also considered in the FEA analysis. It was shown that generally as the layer thickness reduces, the AC resistance reduces as well. When the copper

tracks are wider, the coil AC resistance is more sensitive to the dielectric thickness between the layers. Moreover, it was concluded that the presence of the ferrite material has a negligible effect on the AC resistance. An optimal 4-layer PCB design was selected to replace the Litz wire in the magnetic couplers. To investigate the temperature rise of the proposed printed coil, a thermal analysis based on FEA is presented. It was shown that the maximum temperature of the copper will remain in the safe operating region of the board material.

Finally, a 3.3 kW wireless charging system based on the PCB coil on the secondary side is built. The efficiency of the system versus output power is measured experimentally which showed good accordance with the simulations. It was shown that the proposed PCB coil can replace the vehicle side Litz wire without sacrificing considerable system efficiency.

REFERENCES

[1] H. Feng, R. Tavakoli, Z. Pantic, and O. C. Onar, "Advances in high-power wireless charging systems: Overview and design considerations," *IEEE Trans. Transp. Electrific.*, vol. 6, no. 3, pp. 886–919, Sep. 2020.

[2] D. Patil, M. K. McDonough, J. M. Miller, B. Fahimi, and P. T. Balsara, "Wireless power transfer for vehicular applications: Overview and challenges," *IEEE Trans. Transp. Electrific.*, vol. 4, no. 1, pp. 3–37, Mar. 2018.

[3] S. Li and C. C. Mi, "Wireless power transfer for electric vehicle applications," *IEEE J. Emerg. Sel. Topics Power Electron.*, vol. 3, no. 1, pp. 4–17, Mar. 2015.

[4] M. A. Saket, M. Ordonez, and N. Shafiei, "Planar transformers with near-zero common-mode noise for flyback and forward converters," *IEEE Trans. Power Electron.*, vol. 33, no. 2, pp. 1554–1571, Feb. 2018.

[5] Z. Ouyang and M. A. E. Andersen, "Overview of planar magnetic technology—Fundamental properties," *IEEE Trans. Power Electron.*, vol. 29, no. 9, pp. 4888–4900, Sep. 2014.

[6] J. Qu, L. He, N. Tang, and C. Lee, "Wireless power transfer using domino-resonator for 110-kV power grid online monitoring equipment," *IEEE Trans. Power Electron.*, vol. 35, no. 11, pp. 11380–11390, Nov. 2020.

[7] R. Hua and A. P. Hu, "Modeling and analysis of inductive power transfer system with passive matrix power repeater," *IEEE Trans. Ind. Electron.*, vol. 66, no. 6, pp. 4406–4413, Jun. 2019.

[8] Y. Cho *et al.*, "Thin hybrid metamaterial slab with negative and zero permeability for high efficiency and low electromagnetic field in wireless power transfer systems," *IEEE Trans. Electromagn. Compat.*, vol. 60, no. 4, pp. 1001–1009, Aug. 2018.

[9] C. Yang, C. Chang, S. Lee, S. Chang, and L. Chiou, "Efficient four-coil wireless power transfer for deep brain stimulation," *IEEE Trans. Microw. Theory Techn.*, vol. 65, no. 7, pp. 2496–2507, Jul. 2017.

[10] C. Byungcho, N. Jaehyun, C. Honnyong, A. Taeyoung, and C. Seungwon, "Design and implementation of low-profile contactless battery charger using planar printed circuit board windings as energy transfer device," *IEEE Trans. Ind. Electron.*, vol. 51, no. 1, pp. 140–147, Feb. 2004.

[11] K. Chen and Z. Zhao, "Analysis of the double-layer printed spiral coil for wireless power transfer," *IEEE J. Emerg. Sel. Topics Power Electron.*, vol. 1, no. 2, pp. 114–121, Jun. 2013.

[12] *Wireless Power Transfer for Light-Duty Plug-In/Electric Vehicles and Alignment Methodology*, Standard SAEJ2954, 2020. [Online]. Available: https://www.sae.org/standards/content/j2954_202010/

[13] J. Liu, K. W. Chan, C. Y. Chung, N. H. L. Chan, M. Liu, and W. Xu, "Single-stage wireless-power-transfer resonant converter with boost bridgeless power-factor-correction rectifier," *IEEE Trans. Ind. Electron.*, vol. 65, no. 3, pp. 2145–2155, Mar. 2018.

[14] N. Mohan, T. M. Undeland, and W. P. Robbins, *Power Electronics: Converters, Applications, and Design*. Hoboken, NJ, USA: Wiley, 2003.

[15] R. Bosshard *et al.*, "Modeling and η-α pareto optimization of inductive power transfer coils for electric vehicles," *IEEE J. Emerg. Sel. Topics Power Electron.*, vol. 3, no. 1, pp. 50–64, Mar. 2015.

[16] E. C. W. de Jong, B. J. A. Ferreira, and P. Bauer, "Toward the next level of PCB usage in power electronic converters," *IEEE Trans. Power Electron.*, vol. 23, no. 6, pp. 3151–3163, Nov. 2008.

[17] D. v. d. Linde, C. A. M. Boon, and J. B. Klaassens, "Design of a high-frequency planar power transformer in multilayer technology," *IEEE Trans. Ind. Electron.*, vol. 38, no. 2, pp. 135–141, Apr. 1991.

[18] A. Ramezani and M. Narimani, "Optimized electric vehicle wireless chargers with reduced output voltage sensitivity to misalignment," *IEEE J. Emerg. Sel. Topics Power Electron.*, vol. 8, no. 4, pp. 3569–3358, Dec. 2020.

[19] A. Ramezani, S. Farhangi, H. Iman-Eini, B. Farhangi, R. Rahimi, and G. R. Moradi, "Optimized LCC-series compensated resonant network for stationary wireless EV chargers," *IEEE Trans. Ind. Electron.*, vol. 66, no. 4, pp. 2756–2765, Apr. 2019.

[20] A. Ramezani and M. Narimani, "A new wireless EV charging system with integrated DC-DC magnetic element," *IEEE Trans. Transp. Electrific.*, vol. 5, no. 4, pp. 1112–1123, Dec. 2019.

ALI RAMEZANI (Student Member, IEEE) received the B.Sc. degree in electrical engineering from Shahid Beheshti University, Tehran, Iran, in 2014, the M.Sc. degree in electrical engineering from the University of Tehran, Tehran, Iran, in 2017, and the Ph.D. degree from the Department of Electrical and Computer Engineering, McMaster University, Hamilton, ON, Canada, in 2021. He is currently an Electrical Engineer with eLeapPower, Toronto, ON, Canada. His research interests include wireless power transfer, design and control of the automotive high-power converters, magnetic design, and renewable energy sources.

MEHDI NARIMANI (Senior Member, IEEE) received the Ph.D. degree in electrical engineering from the University of Western Ontario, London, ON, Canada, in 2012. He is currently an Assistant Professor with the Department of Electrical and Computer Engineering, McMaster University, Hamilton, ON, Canada. Prior joining McMaster University, he was a Power Electronics Engineer with Rockwell Automation Canada, Cambridge, ON, Canada. He has authored or co-authored more than 120 journal and conference proceeding papers, coauthored a Wiley-IEEE Press book, and holds seven issued/pending US/European patents. His current research interests include power conversion, high-power converters, control of power electronics converters, fast EV Chargers, and wireless EV charging systems.